Dynamic SPECT Imaging of Dopamine D2 Receptors in Human Subjects with Iodine-123-IBZM

John P. Seibyl, Scott W. Woods, Sami S. Zoghbi, Ronald M. Baldwin, Holley M. Dey, Andrew W. Goddard, Yolanda Zea-Ponce, George Zubal, Mark Germine, Eileen O. Smith, George R. Heninger, Dennis S. Charney, Hank F. Kung, Abass Alavi, Paul B. Hoffer and Robert B. Innis

Departments of Psychiatry and Diagnostic Radiology, Veterans Affairs Medical Center, Yale University School of Medicine, West Haven, Connecticut and the Division of Nuclear Medicine, University of Pennsylvania School of Medicine, Philadelphia, Pennsylvania

We studied the uptake, distribution, metabolism and washout of the dopamine D2 receptor ligand [^{123}I]IBZM in healthy subjects (n = 12) with dynamic brain SPECT. The highest radioactivity level was detected in the striatum. Operationally-defined striatal "specific" uptake peaked at 69 min postinjection of radioligand and showed a gradual decline of 15% per hour thereafter. "Specific" uptake at maximal counts represented 53% of the total striatal radioactivity. Two subjects received haloperidol (20 μg/kg i.v.) 80 min postinjection of radioligand. Haloperidol caused a 2.6-fold increase in the rate of washout of specific striatal activity in comparison to that in the 10 control subjects and was consistent with drug-induced displacement of radioligand from the dopamine D2 receptor. Two classes of metabolites were detected in plasma and urine: a polar fraction, not extracted by ethyl acetate, and a nonpolar, extractable fraction consisting of parent compound and two compounds having shorter retention times on reversed-phase HPLC. Greater than half the plasma parent was metabolized within 10–15 min after administration. The volume of distribution, estimated from the peak arterial plasma concentration at 50–75 sec, was 7.7–10.2 l; the free (nonprotein bound) fraction of [^{123}I]IBZM after in vitro incubation with blood or plasma was 4.4% ± 0.4%. These results suggest that [^{123}I]IBZM exhibits uptake in brain regions with high D2 receptor density and shows a relatively stable washout during which drugs affecting dopaminergic transmission may be administered.

J Nucl Med 1992; 33:1964–1971

Brain imaging of dopamine D2 receptors in humans has been performed with PET (positron emission tomography) using ^{11}C- and ^{18}F-labeled spirodecanone and benzamide compounds (*1,2*). Similar receptor studies have been performed recently with SPECT (single-photon emission computed tomography) using ^{123}I-labeled benzamide analogs (*3–6*). In particular, the iodobenzamide IBZM (S-(−)-N-[(1-ethyl-2-pyrrolidinyl) methyl]-2-hydroxy- 3-iodo-6-methoxybenzamide) has been radiolabeled with ^{125}I for homogenate binding studies and with ^{123}I for SPECT brain imaging. Iodine-125-IBZM binding to striatal tissue homogenate showed pharmacological selectivity for dopamine D2 receptors (compared with D1 sites), saturability (with Bmax or number of binding sites = 480 fmole/mg rat striatum), reversibility by displacing agents, high affinity (Kd or dissociation constant = 0.43 n*M*), and stereoselectivity (with the S-isomer 300-fold more potent than the R-isomer (*3*). SPECT imaging in non-human primates has been consistent with the successful in vitro labeling of dopamine D2 receptors and shown highest uptake in striatum with displacement by the high affinity D2 receptor agent haloperidol (*5,7*). Recent extension of these studies to human subjects have similarly shown high striatal activity and blockade of uptake by pretreatment with neuroleptic medications (*8,9*).

Several physical characteristics of SPECT imaging with ^{123}I-labeled tracers may limit its ability to provide useful receptor data relative to comparable PET studies. For example, the lower sensitivity of SPECT would tend to decrease its dynamic capabilities by increasing the necessary sampling time per image acquisition, with the injected dose limited by radiation safety guidelines. The purpose of the present study was to gain additional information on the dynamic capabilities of SPECT dopamine receptor imaging in human subjects. In particular, serial SPECT scans and arterial blood measurements of radiolabeled metabolites were obtained to assess dynamic aspects of the uptake and washout of brain activity. The reversibility and pharmacological selectivity of brain activity was measured by haloperidol-induced displacement of activity, in distinction to pretreatment blockade of uptake.

Received Nov. 8, 1991; revision accepted Jul. 1, 1992.
For reprints contact: John P. Seibyl, MD, Psychiatry Service 116A, West Haven VA Medical Center, 950 Campbell Ave., West Haven, CT 06516.

METHODS

Subjects

Twelve healthy subjects (9 males, 3 females; age 26.5 ± 3.7 yr, weight 76.3 kg ± 14.1 kg, with these and all subsequent data expressed as mean ± s.d.) participated in the study after giving informed consent. Subjects were free of medical or psychiatric illness and had no family history of psychiatric illness on the basis of a structured interview with a research psychiatrist, physical examination, laboratory screening studies and EKG. Female subjects had a negative serum β-HCG performed on the day of SPECT scanning.

Radiolabeling

Iodine-123-IBZM was prepared by a oxidative radioiodination of the noniodinated precursor, BZM (S-(−)-N-[(1-ethyl-2-pyrrolidinyl)methyl]-2-hydroxy-6-methoxybenzamide), with no-carrier-added [^{123}I]NaI, using the peracetic acid technique of Kung et al. (*10*). The labeled product, [^{123}I]IBZM, was separated from unreacted BZM and small amounts of impurities by elution from an HPLC C-18 reverse-phase column (PRP-1, Hamilton) using isocratic 82% acetonitrile/4 m*M* phosphate buffer, pH 7.0 and a flow rate of 1.0 ml/min. The final product was formulated in sterile saline, sterilized by membrane filtration (0.2 μm) and confirmed to be pyrogen-free prior to its use. The radiochemical purity of the product (Rt = 18 min) was 94.6% ± 2.1%. The specific activity was too high to measure the small amount of carrier present.

Imaging Procedure

Studies were performed on the 810X brain Imager (Strichman Medical Equipment, Medfield, MA). This device uses focused collimation to obtain single transaxial slices with a resolution measured as the FWHM of the point spread function of approximately 8 mm in-plane and 13 mm in the z-axis (*11,12*). Subjects received stable iodide premedication (150 mg KI) administered 1 hr (first four subjects) and 24, 7 and 1 hr (next eight subjects) before the radiopharmaceutical infusion to block thyroid uptake. The subjects' heads were aligned with a laser light for obtaining images parallel to the canthomeatal (CM) line. Iodine-123-IBZM (4.9 ± 0.5 mCi) was injected via an antecubital vein over approximately 10 sec. Subjects remained in the quiet, dimly lit scanning room with eyes and ears unblocked for the duration of the scan. Initial 1-min single images were obtained every 5 mm in planes parallel to the CM line. These images were reconstructed and attenuation-corrected assuming uniform attenuation equal to water for an ellipse drawn around the brain. Visual inspection of these early images permitted selection of the slice that overlay the striatum. Subsequent images from repeated 3–6 min data acquisitions were obtained from the chosen striatal slice until the end of the study 129 ± 39 min after [^{123}I]IBZM injection.

Two subjects received haloperidol (20 μg/kg, equal to 50 nmol/kg, i.v. over 60 sec) at 80 min postinjection of [^{123}I]IBZM, and images were acquired for the subsequent 60 min. Both subjects received intravenous diazepam (5–10 mg) at 8–15 min posthaloperidol injection for treatment of akathisia.

Arterial Blood Sampling and Metabolite Analysis

Arterial plasma metabolites were measured in six subjects. Serial arterial blood samples were taken in heparin-treated syringes and stored at 4°C until analyzed. Control experiments demonstrated stability of the product for at least 24 hr under these conditions. The plasma was separated by centrifugation and aliquots were assayed in a calibrated gamma counter to measure the total radioactivity. For the metabolite analysis, the plasma was extracted three times with equal volumes of ethyl acetate and the extractable activity was calculated. The organic solvent was evaporated and the residue was taken up in ethanol and analyzed by HPLC on a PRP-1 reversed-phase column with acetonitrile/4 m*M* ammonium phosphate, pH 7 (82:18 v/v) at a flow rate of 1.0 ml/min; 25 × 1 ml fractions were collected and counted in the gamma counter. Controls were run each time by adding the subject's blood to an aliquot of labeled product at the time of administration and to the other aliquot at the time of analysis (15–18 hr later). These samples confirmed the stability of the compound and served to calibrate the HPLC system. Protein binding was determined in vitro by incubating the ^{123}I ligand with plasma and whole blood and subjecting to a 200-μl aliquot to centrifugal ultrafiltration membranes having a 30,000 molecular weight cut-off (Centricon-30, Amicon Division, W.R. Grace & Co., Danvers, MA). The free (unbound) fraction was obtained by the ratio of the activity in the filtrate to the total.

Image and Data Analysis

All images from a single study were reconstructed with a fixed filter, selected using the software provided with the 810X Brain Imager (version 2.6) for the striatal slice in the study with the highest total counts. This method of fixed filter reconstruction was used to eliminate variability associated with the software program's automatic selection of different filters based upon the total counts in each slice.

Regions of interest (ROIs) were drawn on reconstructed images by outlining areas corresponding to left and right striatum, frontal and occipital regions (Fig. 1). This ROI template was then applied to all images in that study. Regional activity was measured in units of counts/pixel/min determined by dividing the total counts in the ROI by the area in pixels and by the acquisition time in minutes. Each pixel corresponded to an area of approximately 1.6 × 1.6 mm. Units of activity cannot be directly expressed as Bq or moles/gm tissue due to inherent problems in quantification of SPECT, but they do represent units linear with concentrations of radioactivity, verified with phantom studies on the 810X Brain Imager (*13*). All activity measurements were decay-corrected to the time of radioligand injection. Right and left striatal activities were averaged and were thought to represent receptor bound radioligand (i.e., specifically bound) plus nonspecifically-bound and free radioactivity. Because of the very low density of dopamine D2 receptors in neocortical areas (*14*), occipital activity was assumed to represent nonspecifically bound and free radioactivity. Thus, specifically bound radioligand was operationally defined as striatal activity minus occipital activity. The validity of this method of data analysis, which is also used by Innis et al. (*7*) and Brücke et al. (*9*), is dependent on future studies showing that free and nonspecifically bound activities are equal in striatum and cortical regions.

The peak of the time-activity curve was determined for each brain region by selecting the time point with the highest count density. Rates of washout of regional brain activity were determined using all data points after the time of peak uptake with a graphics software program (Kaleidagraph® 2.1, Synergy Software, Reading, PA). Washout rates were calculated from both a least squares linear fitting (with rate expressed as % initial value/hr) and a first order exponential fitting (with rate expressed as $T_{½}$ value in min).

RESULTS

Brain Uptake

Subjects received intravenous [^{123}I]IBZM at an average dose of 4.9 ± 0.5 mCi, with these and all data expressed as mean ± s.d. Highest uptake overlay the striatal areas, which formed bilaterally symmetrical ROIs in a plane parallel and 5.6 ± 0.5 cm superior to the CM line (Fig. 1). Striatal activity reached maximal values at 44.7 ± 9.1 min postinjection of radioligand (Table 1). Activities in frontal and occipital areas peaked at 24.5 ± 16.3 min and 18.6 ± 17.2 min, respectively, and were significantly earlier than that in striatum ($p < 0.001$ and $p < 0.0001$, respectively, two-tailed t-test). The operationally defined "specific" uptake (equal to the striatal minus occipital) reached maximal values at 66.5 ± 13.7 min (Table 1). At this time point of maximal "specific" uptake, 52.8% ± 6.2% of the striatal values represented "specific" activity.

Washout of Brain Activity

Washout of regional brain activity was analyzed with both a least square linear and an exponential fitting of all data points subsequent to the time of maximal values in that region. For the linear data fitting the washout of striatal activity (14.1% ± 6.3%/hr) was not significantly different from that of specific activity (15.5% ± 9.4%), ($p = 0.733$, two-tailed t-test) (Table 2). However, the washout of frontal (27.5% ± 4.0%/hr) and occipital areas (24.2 ± 4.3%/hr) were significantly faster than that in striatum ($p < 0.0001$, $p < 0.0001$, respectively).

In general, similar effects were found for the exponential fitting of data points. The half-life for washout of striatal activity (219 ± 108 min) and specific activity (402 ± 318 min) were not significantly different ($p = 0.16$). Washout half-life of frontal (102 ± 28 min) was significantly faster than that in striatum ($p = 0.005$), but that in the occipital region (156 ± 86 min) was not significantly faster than striatum ($p = 0.19$). However, frontal and occipital washout half-lives were significantly faster than "specific" striatal washout ($p = 0.01$ and $p = 0.05$, respectively).

To assess the effect of the size of the ROI on calculated washout rates, large (450–600 pixels) and small (40–60 pixels) striatal regions were compared directly in the first 10 subjects (Table 3). Washout rates calculated from a least squares linear fitting the data for small (21.8% ± 18.7%/hr) versus a large (15.5% ± 9.4%/hr) ROI were not statistically different ($p = 0.34$).

Effect of Haloperidol

Administration of haloperidol (20 μg/kg) at 80 min postradioligand injection increased the washout rate of striatal activity (Figs. 3 and 4). In the two subjects tested, washout rates determined by a linear fit to the points post haloperidol injection of both striatal (32%/hr) and "specific" (39.5%/hr) activities were significantly greater than that of the 10 control subjects ($p = 0.003$ and $p = 0.009$, respectively, two-tailed Student's t-test). However, the administration of haloperidol had no significant effect on washout rates in frontal ($p = 0.52$) and occipital ($p = 0.22$) regions compared to the control group. Within-haloperidol subject analyses of striatal washout rates 30 min prior and posthaloperidol injection showed increased washout after neuroleptic (from 6.3% to 56% for Subject 11, and 7.5% to 38% for Subject 12). Injection of haloperidol induced subjective symptoms of akathisia characterized by psychomotor restlessness, hot/cold flashes, a compulsion to move, and uneasiness. Both subjects received diazepam (5–10 mg i.v.) 8–15 min after haloperidol infusion.

Metabolism and Protein Binding

In two subjects in whom early sampling was carried out, peak arterial plasma concentration was reached 50–75 sec after administration; the volume of distribution, estimated from the peak concentration, was 7.7–10.2 liter. The concentration of total ^{123}I in the venous plasma paralleled that in the arterial plasma within 10–12 min after administration. Solvent extraction and high-pressure liquid chromatography (HPLC) of the plasma revealed two classes of metabolites; a polar fraction, not extracted by ethyl acetate, and a nonpolar, extractable fraction. HPLC analysis of the extract separated this fraction into parent compound "A", with a retention time (Rt) of 11.2 ± 0.1 ($n = 6$), and two lipophilic metabolites: "B", Rt 7.9 ± 0.1 ($n = 6$) and "C", Rt 3.2 ± 0.03 ($n = 6$). The composition changed from mostly parent compound immediately after administration to less than 50% parent within 10–15 min (Fig. 5). The major activity remaining in the plasma was accounted for by the polar fraction "D", which increased rapidly for the first hour to about 80% of the plasma activity. The contribution of the short retention time lipophilic metabolite C increased to about 15% of the plasma activity at 20–30 min and then declined. The intermediate component B was clearly observed in two of the six subjects, peaking at 5–10 min postinjection at 20%–40% of the plasma activity. In two other subjects, component B appeared in some samples but appeared to be incompletely resolved from the parent peak in others. The modification of the mobile phase to use 3,3-dimethylglutarate as the buffer instead of phosphate (*5*) did not change the pattern. In the remaining two subjects, there was no indication of metabolite B.

In one subject, urine collected at 110 min postinfusion was analyzed using the same technique as for the plasma: the composition was 0.4% A (parent), 1.8% C, and 97.8% not extractable. Control experiments showed that [^{123}I]IBZM was 93.7% extracted and [^{123}I]NaI was 5.4% extracted when added to nonradioactive urine and treated in the same way.

Protein binding of [^{123}I]IBZM determined by ultrafiltration demonstrated a free fraction (not protein bound) of 4.4% ± 0.4% ($n = 8$) for in vitro incubation with whole blood either immediately or overnight and with plasma; the whole blood and plasma values were within 0.1% of each other.

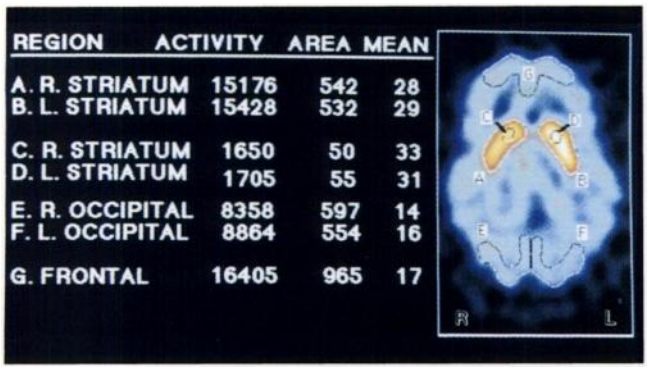

FIGURE 1. Transaxial SPECT image obtained at level of the striatum with [^{123}I]IBZM in a control subject 76 min postinjection of radioligand. This image was reconstructed from data acquired by the Strichman 810X over 6 min in a plane parallel to and 5.0 cm above the canthomeatal line. A typical ROI template for radioactivity measurements is superimposed on the image. The figure showed right (R) and left (L) regions from the striatum and occipital region and bilateral frontal region. The "mean" regional activity is equal to the activity in the region divided by the number of pixels and acquisition time in minutes.

TABLE 1
Time to Maximal Activity (min Post-[^{123}I]IBZM Injection) During Dynamic SPECT

Control subjects	Time of peak activity				Percent "specific" binding at peak (striatal)
	Frontal	Occipital	Striatal	"Specific"	
1	10	10	48	48	51
2	16	16	39	76	53
3	20	20	42	79	46
4	4	4	46	76	57
5	20	8	57	79	49
6	28	28	47	47	60
7	63	63	63	63	43
8	32	9	32	67	49
9	33	9	56	68	61
10	19	19	47	71	59
Mean	24.5	18.6	47.7	67.4	52.8
s.d.	16.3	17.2	9.1	11.7	6.2
Haloperidol subjects					
11	34	18	43	82	42.4
12	24	24	42	56	55
Mean	29	21	42.5	69	48.7
s.d.	7.1	4.2	0.7	18.4	8.9

Regional brain analyses of time to peak activity and percent "specific" activity in striatum at maximum activity (defined as [total striatal activity minus occipital activity]/total striatal activity × 100) for 10 control subjects and 2 haloperidol subjects.

DISCUSSION

These data demonstrate the feasibility of [^{123}I]IBZM dynamic SPECT brain imaging in humans. Maximal activity occurred in the striatum and washed out at 15.5% per hour. Administration of haloperidol in two subjects increased the washout of the striatal specific uptake, consistent with drug-induced displacement of radioligand from the D2 receptor. The major metabolic fate of [^{123}I] IBZM is to polar metabolites, while the ethyl acetate extractable portion of plasma revealed parent compound was rapidly, but variably metabolized to at least two less lipophilic compounds.

Brain uptake has been referred to as "activity", since the radiochemical identity of the source of brain emissions has not been determined in primate brain. In rodents, re-extraction models of [^{123}I]IBZM support the idea that only the parent compound enters the brain (*3*) and that prepared metabolites, which are more polar, do not cross the blood-brain barrier (Kung, unpublished results). Preliminary results in a baboon (Papio anubis) from our lab suggest that extractable activity in the brain was >88% parent compound. The present human study demonstrates that [^{123}I]IBZM is variably metabolized to one or two metabolites which are more polar than the parent compound. Further characterization of these metabolites from human plasma will be required to demonstrate they do not enter the brain.

Brain activity showed regionally specific variation in both time to peak levels and rates of washout, which are consistent with the distribution of dopamine D2 receptors. Considering pharmacodynamic factors, a region rich in receptors like the striatum constitutes a relatively large "reservoir" for uptake of radioligand and would, therefore, have a prolonged time to reach maximal activity. Receptor-rich regions would also be predicted to have slower washout rates than receptor-poor regions and to demonstrate displacement by D2 receptor antagonists. These predictions based on in vivo kinetic modeling were demonstrated in this study with dynamic SPECT imaging. Furthermore, similar washout rates of striatal and "specific" striatal activity suggest the majority of signals from this region are derived from the receptor-bound activity. Other factors, including variable pharmacokinetics in different brain regions, may also be implicated in the variable time to peak and radioactivity washout rates in different brain regions.

It is possible that haloperidol-induced washout of striatal activity in the present study may have been caused both directly by haloperidol itself and indirectly via released dopamine. SPECT imaging studies of [^{123}I]IBZM in monkeys support the idea that endogenous dopamine may effectively compete with radioligand for binding to the D2 receptor (*7*). Administration of the dopamine-releasing agent d-amphetamine caused an increased washout of striatal activity. This effect of d-amphetamine, but not that of haloperidol, was blocked by prior treatment of animals with reserpine, which depletes tissue stores of dopamine. The dose of haloperidol used for these monkey experiments (20 μg/kg i.v.) was the same as that used in the human studies. The animal experiments suggest that some, but not necessarily all, the actions of haloperidol are

TABLE 2
Regional Brain Activity Washout

Control subject	Percent washout per hour and r value of linear fit								Half-Life in min and r value of exponential fit							
	Frontal	r	Occipital	r	Striatal	r	"Specific"	r	Frontal	r	Occipital	r	Striatal	r	"Specific"	r
1	25	0.95	21	0.92	10	0.62	7	0.2	136	0.88	253	0.63	355	0.63	611	0.21
2	30	0.95	28	0.97	9	0.78	8	0.223	94	0.95	104	0.97	423	0.82	120	0.76
3	30	0.96	24	0.95	12	0.79	13	0.27	93	0.95	133	0.91	286	0.79	360	0.42
4	21	0.9	21	0.97	13	0.9	10	0.49	163	0.8	146	0.94	254	0.89	907	0.23
5	25	0.9	18	0.87	2	0.14	36	0.71	104	0.88	353	0.16	102	0.98	55	0.72
6	23	0.88	20	0.94	17	0.98	16	0.92	104	0.94	112	0.97	136	0.98	157	0.92
7	26	0.95	26	0.96	20	0.88	6	0.23	84	0.96	91	0.97	138	0.89	510	0.24
8	32	0.97	28	0.98	24	0.98	23	0.82	76	0.99	93	0.99	117	0.97	173	0.76
9	32	0.89	32	0.92	18	0.93	13	0.66	80	0.87	94	0.83	180	0.94	905	0.22
10	31	0.96	24	0.88	16	0.94	23	0.73	81	0.94	179	0.76	202	0.94	219	0.6
Mean	27.5	0.93	24.2	0.94	14.1	0.79	15.5	0.5	101.5	0.92	155.8	0.81	219.3	0.9	401.7	0.5
s.d.	4.0	0.0	4.3	0.0	6.3	0.3	9.4	0.3	27.8	0.1	85.7	0.3	108.1	0.1	318.2	0.3
Haloperidol subject																
11	24	0.92	20	0.99	32	0.93	47	0.7	102	0.79	129	0.91	57	0.91	18	0.86
12	27	0.74	20	0.91	32	0.88	32	0.88	85	0.89	126	0.93	115	0.86	103	0.59
Mean	25.5	0.83	20	0.95	32	0.9	39.5	0.79	93.5	0.84	127.5	0.92	86	0.88	60.5	0.72
s.d.	2.1	0.1	0.0	0.1	0.0	0.0	10.6	0.1	12.0	0.1	2.1	0.0	41.0	0.0	60.1	0.2

Percentage activity washout per hour after peak maximal activity. Washout was determined from a least squares linear and exponential fitting to time points subsequent to the maximal activity in that region. For haloperidol subjects, washout was calculated for data points obtained after haloperidol administration (approximately 80 min).

TABLE 3
Effect of Region of Interest Size on Striatal "Specific" Washout Rates

Subject	Striatal Washout Rate (% per hr)			
	Large ROI	r	Small ROI	r
1	7	0.21	64	0.16
2	8	0.22	5	0.06
3	13	0.28	33	0.28
4	10	0.48	12	0.61
5	36	0.71	28	0.79
6	16	0.92	15	0.87
7	6	0.24	2	0.1
8	23	0.83	25	0.8
9	13	0.66	4	0.21
10	23	0.73	30	0.8
Mean	15.5	0.53	21.8	0.47
s.d.	9.4	0.27	18.7	0.33

Effect of a large (450–600 pixel) ROI versus a small (~50 pixel) ROI on "specific" activity washout rate in striatum. No differences are noted in large vs. small ROI in rates of washout calculated from a least squares linear fitting to the data points.

mediated directly by drug-induced displacement of radioligand, since acute injection of haloperidol in rodents has been shown to cause an increase in extracellular dopamine levels (*15*).

This dynamic brain SPECT data suggests the feasibility of analysis using standard two or three compartment kinetic models. However, obstacles in applying this data to such analysis include: (1) the accuracy of attenuation and scatter correction; (2) the correction of partial volume errors; (3) the lack of early data points that characterize the K_1; (4) the poor target-to-background signal and the precision of methods for estimating the receptor-associated radioactivity; and (5) the incomplete characterization of metabolites.

Accurate scatter and attenuation correction of SPECT data is required to convert counts/min/pixel into absolute units of activity (e.g., μCi/ml) using numerical conversion factors derived from brain phantoms. No established method exists for attenuation correction of individual subjects based on a transmission scan, as is commonly performed in PET, although preliminary work in both brain and cardiac SPECT suggests the feasibility of performing these corrections (*16,17*). Partial volume errors may be significant in the striatum with D2 agents. The effects of partial voluming can be seen in the comparison of large versus small sized ROIs drawn in striatum where the smaller ROIs have 13% greater activity than the larger ROIs. However, the smaller ROIs, while overall more accurate, are more subject to head movement and provide noiser time-activity data.

The use of a single slice camera in generating the present data set limited the number of early time points, as the majority of images were obtained at slice levels that were not subsequently imaged. The "best" striatal slice was localized by acquiring images at different levels until the striatum was well visualized. This process required 25–30 min in most subjects and resulted in fewer early points that define the brain tracer uptake (K_1). In the future, the

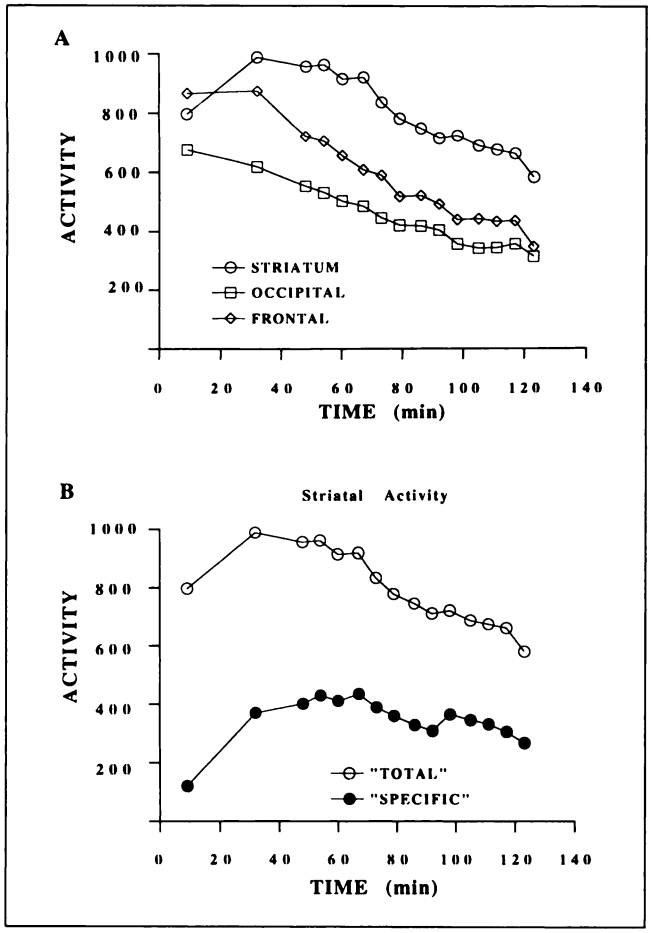

FIGURE 2. Regional brain time-activity curve for [^{123}I]IBZM in a control subject. Radioactivity is expressed as counts/pixel/min with each pixel corresponding to approximately 1.6 × 1.6 mm. Brain time-activity curves (a) show activity in striatum, occipital and frontal cortex and (B) total striatal activity and operationally-defined "specific" striatal activity determined by subtraction of occipital activity from striatal activity in each acquisition.

SPECT slice level may be chosen on the basis of CT or MRI, or multislice SPECT devices can be employed to collect these early points.

Another consideration in the application of this data to kinetic models is the poor target-to-background signal with [^{123}I]IBZM resulting in the need to estimate the contribution of brain signal from activity bound at the receptor. We employed a crude estimate of this activity by subtracting the radioactivity in the posterior cortical region from the total striatal counts. This assumes the nonspecific binding is equal in both regions. An alternative approach is to estimate the amount of displaceable activity by injecting a displacing agent like haloperidol. By assuming that haloperidol causes enhanced striatal washout by directly binding to the receptor, a dose of the drug that occupies all receptor sites will displace all the bound activity. In the present work, the injection of haloperidol caused a reduction of striatal activity to about the level of other cortical regions and had no effect on extrastriatal brain regions suggesting the feasibility of this method for estimating receptor-associated radioactivity. Agents with higher target-to-background ratios, while having less error associated with the estimation of specific bound radioactivity, will pose greater partial volume error.

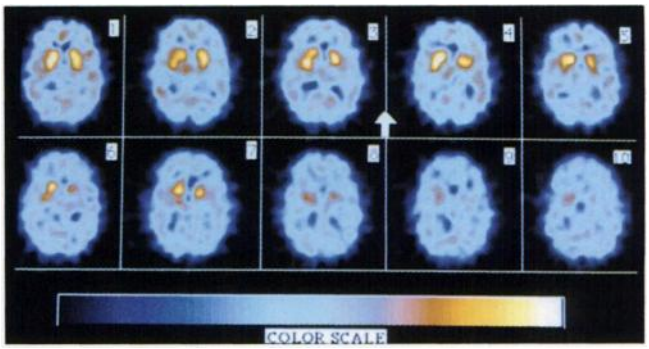

FIGURE 3. Serial [^{123}I]IBZM dynamic SPECT images acquired every 2 min through the same plane in subject receiving haloperidol. Between slices 3 and 4 (indicated by the arrow), the administration of haloperidol 20 μg/kg i.v. caused a rapid decrease of radioactivity from the brain. This washout is consistent with displacement of radioligand bound to the dopamine receptor.

Further development of SPECT kinetic modeling will also require measurement of the input function and methods for assaying free parent compound in arterial plasma. Initial results of the metabolic fate of injected [^{123}I]IBZM are described in this paper and have previously been reported by Kung et al. (*5*). In this larger sample, we find the variable presence of a second minor lipophilic metabolite that elutes close to the parent compound. By comparison, the atypical benzamide antipsychotic remoxipride has been reported to have two relatively lipophilic metabolites (*18*). For IBZM, the major metabolic pathways are to polar metabolites; our present methods do not allow distinguishing between ionic [^{123}I]iodide and glucoronides and/or oxygenated metabolites, analogous to other benzamide neuroleptics (*19*). The significance of these metabolites with regard to effects at brain D2 receptors requires further characterization.

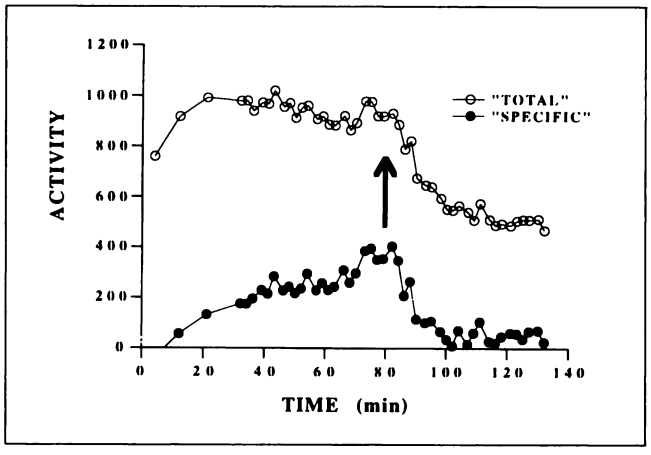

FIGURE 4. Time-activity curve for the subject in Figure 3 shows the effect of haloperidol on striatal and "specific" activity washout rate.

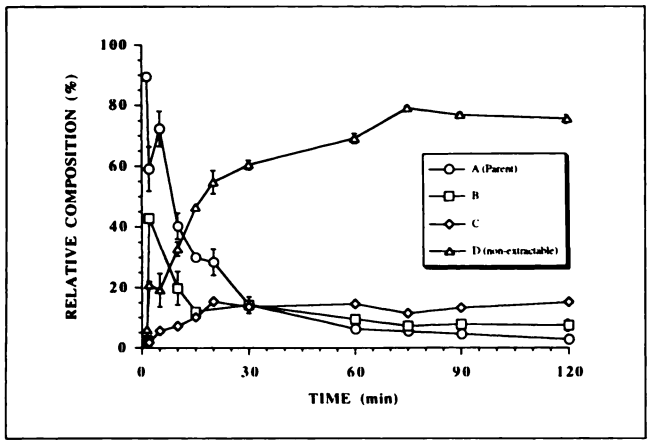

FIGURE 5. The relative composition of arterial plasma in six normal human volunteers after administration of [^{123}I]IBZM, determined by ethyl acetate extraction and HPLC. Values at each time point are expressed as the relative areas under the HPLC peaks multiplied by their respective extraction efficiencies from plasma. Circle = parent compound "A", Rt 11.2 min; square = lipophilic metabolite "B", Rt 7.9 min; diamond = lipophilic metabolite "C", Rt 3.2 min; triangle = polar metabolite fraction "D", not extracted by ethyl acetate. Error bars are standard error of the mean for those time points where more than one subject was measured.

In light of the obstacles to accurate kinetic modeling with SPECT, between-subject experimental designs may provide the most conservative semiquantitative paradigm. For example, within-subjects experimental designs will be less vulnerable to inaccuracies of attenuation correction provided that the head is maintained in a fixed position during the scan and identical ROIs are used for each image of the study. In this manner, changes in a particular region would provide meaningful and quantitative data (expressed as % change), since we have previously shown that activity within fixed ROIs are linear with concentrations of radioactivity (*13*). For dramatic changes as with haloperidol, displacement of [^{123}I]IBZM showed significant effects even with a between-subjects comparison (Table 2). However, for more subtle effects, like that potentially of d-amphetamine-induced displacement of [^{123}I]IBZM, a within-subject design would be expected to be more sensitive and perhaps more accurate as it obviates the individual differences in attenuation correction. For this reason, we also analyzed the washout rate in the haloperidol-injected subjects in the 30-min period before and 30-min period after neuroleptic administration. As described above, this analysis showed a pronounced increase of washout rate in these two subjects and could be used as a typical within-subject design for future [^{123}I]IBZM studies.

Thus, certain experimental SPECT paradigms may require a within-subjects design. Since the effects of pharmacological or even behavioral interventions will probably be assessed relative to changes in washout rates of the radioligand, we have presented and compared linear and first order exponential fittings of the washout data. Modeling theory suggests that brain washout of activity generally follows an exponential function. However, washout is dependent upon several factors, including the rate of metabolism, penetration of blood-brain barrier and whole body clearance, which may result in a nearly linear washout function. Our results cannot distinguish whether a linear or exponential fitting more accurately represents the data. The duration of data sampling may have been too short to distinguish these two possibilities, and future studies may be able to use both methods to assess the effects of pharmacological interventions.

Two final caveats are important in dopamine D2 receptor imaging with [^{123}I]IBZM. The first of these are the effects of age and gender on D2 receptor density and the possibility that alterations in receptor number might affect striatal washout rates. Human postmortem studies and in vivo PET imaging have shown that normal aging is associated with a reduction of striatal D2 density of approximately 2.2% per decade (*1,20*). All subjects in this study were in the third or fourth decades of life and therefore lack adequate variation to assess the effects of age on striatal washout rate. Gender effects may also be relevant to these studies as in vitro models show potent effects of estrogen on D2 receptor number (*21,22*). The three female subjects in this study were in the late luteal phase of the menstrual cycle, a period of falling estrogen levels. Future studies may need to carefully assess the effects of age and menstrual cycle on [^{123}I]IBZM SPECT imaging D2 receptors.

The second caveat relates to the existence of additional recently discovered dopamine receptors, including the D3, D4 and D5 subtypes (*23–25*). Like the related benzamide compound raclopride (*23*), IBZM has significant affinity for the D3 receptor. The distribution and functional significance of these additional dopamine receptor subtypes in humans as well as full characterization of binding of [^{123}I]IBZM to dopamine receptor subtypes remains to be established.

In summary, this study demonstrates the utility of employing [^{123}I]IBZM in dynamic SPECT brain imaging of human D2 receptors. The long half-life and relatively slow period of washout underscore the feasibility of novel strategies for studying brain dopamine function in humans during [^{123}I]IBZM SPECT imaging, including the injection of pharmacological agents which modulate dopaminergic neurotransmission.

ACKNOWLEDGMENTS

This work was supported by funds from the Department of Veterans Affairs (VA Schizophrenia Research Center and Merit Review Award to RBI) and from the Public Health Service (R18 DA06190, P50 DA04060, MH44866, and MH25642). The authors gratefully acknowledge the expert assistance of Gary Wisniewski with the SPECT studies.

REFERENCES

1. Wong D, Wagner H, Dannals R, et al. Effects of age on dopamine and serotonin receptors measured by positron emission tomography in the living human brain. *Science* 1984;226:1391–1396.
2. Farde L, Hall H, Ehrin E, et al. Quantitative analysis of D2 dopamine receptor binding in the living human brain with PET. *Science* 1986;231:258–261.
3. Kung H, Pan S, Kung M-P, et al. In vitro and in vivo evaluation of [^{123}I] IBZM: a potential CNS D-2 dopamine receptor imaging agent. *J Nucl Med* 1989;30:88–92.
4. Brücke T, Tsai Y, McLellan C, et al. In vitro binding properties and autoradiographic imaging of 3-iodobenzamide ([^{125}I]IBZM): a potential imaging ligand for D-2 dopamine receptors in SPECT. *Life Sci* 1988;42:2097–2104.
5. Kung H, Alavi A, Chang W, et al. In vivo SPECT imaging of CNS D-2 dopamine receptors: initial studies with iodine-123 IBZM in humans. *J Nucl Med* 1990;31:573–579.
6. Kessler R, Votaw J, DePaulis T, et al. Iodine-123-labelled epidepride SPECT studies of dopamine D2 receptors in man. *J Nucl Med* 1990;31:779.
7. Innis R, Malison R, Al-Tikriti M, et al. Amphetamine-stimulated dopamine release competes in vivo for [^{123}I]IBZM binding to be D2 receptor in non-human primates. *Synapse* 1992;10:177–184.
8. Costa D, Verhoeff N, Cullum I, et al. In vivo characterisation of 3-iodo-6-methoxybenzamide ^{123}I in humans. *Eur J Nucl Med* 1990;16:813–816.
9. Brücke T, Podreka I, Angelberger P, et al. Dopamine D2 receptor imaging with SPECT: studies in different neuropsychiatric disorders. *J Cereb Blood Flow Metab* 1991;11:220–228.
10. Kung M-P, Kung H. Peracetic acid as a superior oxidant for preparation of [^{123}I]IBZM; a potential dopamine D-2 receptor imaging agent. *J Lab Compd Radiopharm* 1990;27:691–700.
11. Moore S, Mueller S. Inversion of the 3D Radon transform for a multidetector, point-focused SPECT brain scanner. *Phys Med Biol* 1986;31:207–221.
12. Stoddart H. New multidimensional reconstructions for the 12-detector, scanned focal point, single photon tomograph. *Phys Med Biol* 1992;37:579–586.
13. Innis R, Al-Tikriti M, Zoghbi S, et al. SPECT imaging of the benzodiazepine receptor: feasibility of in vivo potency measurements from stepwise displacement curves. *J Nucl Med* 1991;32:1754–1761.
14. Lidow M, Goldman-Rakic P, Rakic P, Innis R. Dopamine D2 receptors in the cerebral cortex: distribution and pharmacological characterization with ^{2}H-raclopride. *Proc Natl Acad Sci* 1989;86:6412–6416.
15. Moghaddam B, Bunney B. Acute effects of typical and atypical neuroleptics on the release of dopamine from prefrontal cortex, nucleus accumbens, and striatum of the rat: an in vivo microdialysis study. *J Neurochemistry* 1990;54:1755–1760.
16. Murase K, Tanada S, Ooie Y, et al. Improvement of brain SPECT quantitation using simultaneous emission and transmission data acquisition in a 4-head SPECT scanner [Abstract]. *J Nucl Med* 1992;32:1066.
17. Gilland D, Jaszczak R, Coleman R. Effects of non-uniform attenuation compensation in SPECT using acquired transmission data [Abstract]. *J Nucl Med* 1991;32:1067.
18. Gawell L, Hagberg C, Hogberg T, Widman M. Synthesis of 5-substituted 5-hydroxy-2-pyrrolidones, metabolites of the antipsychotic benzamide remoxipride. *Acta Chem Scand* 1989;43:476–480.
19. Högberg, Rämsby S, Ogren S, et al. New selective dopamine D2 antagonists as antipsychotic agents. Pharmacological, chemical, structural and theoretical considerations. *Acta Pharm Suec* 1987;24:289–328.
20. Seeman P, Bzowej N, Guan H, et al. Human brain dopamine receptors in children and aging adults. *Synapse* 1987;1:399–404.
21. Van Hartesveldt C, Joyce J. Effects of estrogen on the basal ganglia. *Neurosci Biobeh Rev* 1986;10:1–14.
22. Fernandez-Ruiz J, Armor J, Ramos J. Time-dependent effects of estradiol and progesterone on the number of striatal dopaminergic D2 receptors. *Brain Res* 1989;476:388–395.
23. Sokoloff P, Giros B, Martres M-P, Bouthenet M-L, Schwartz J-C. Molecular cloning and characterization of a novel dopamine receptor D3 as a target for neuroleptics. *Nature* 1990;347:146–151.
24. Van Tol H, Bunzow J, Guan H, et al. Cloning of the gene for a human dopamine D4 receptor with high affinity for the antipsychotic clozapine. *Nature* 1991;350:610–614.
25. Sunahara R, Guan H, O'Dowd B, et al. Cloning of the gene for a human dopamine D5 receptor with higher affinity for dopamine than D1. *Nature* 1991;350:614–619.